

# SAMDWICH: Moment-aware Video-text Alignment for Referring Video Object Segmentation

Seunghun Lee<sup>1\*</sup>, Jiwan Seo<sup>1\*</sup>, Jeonghoon Kim<sup>1\*</sup>, Siwon Kim<sup>1</sup>, Haeun Yun<sup>1</sup>, Hyogyong Jeon<sup>1</sup>, Wonhyeok Choi<sup>1</sup>, Jaehoon Jeong<sup>1</sup>, Zane Durante<sup>2</sup>, Sang Hyun Park<sup>1</sup>, Sunghoon Im<sup>1</sup>,

<sup>1</sup>DGIST, Daegu, Republic of Korea <sup>2</sup>Stanford University, Stanford, CA, USA

## Abstract

Referring Video Object Segmentation (RVOS) aims to segment and track objects in videos based on natural language expressions, requiring precise alignment between visual content and textual queries. However, existing methods often suffer from semantic misalignment, largely due to indiscriminate frame sampling and supervision of all visible objects during training—regardless of their actual relevance to the expression. To address this, we introduce a moment-aware RVOS framework named SAMDWICH, along with a newly annotated dataset, MeViS-M, built upon the challenging MeViS benchmark. We manually annotate temporal moments indicating when each object is referred to by the expression, enabling semantically grounded supervision that strengthens video-text alignment. SAMDWICH leverages these aligned text-to-clip pairs to guide training, significantly enhancing referential understanding. Building upon this framework, we propose Moment-guided Dual-path Propagation (MDP), a moment-aware propagation strategy that improves both object grounding and tracking by training on both relevant and irrelevant frames through a moment-centric memory mechanism. In addition, we introduce Object-level Selective Supervision (OSS), an object-level filtering strategy that supervises only the objects temporally aligned with the expression in each training clip. This selective supervision reduces semantic noise and reinforces language-conditioned learning. Extensive experiments show that SAMDWICH achieves state-of-the-art performance on challenging MeViS benchmark. We will make our code and the MeViS-M dataset publicly available. Project page: [this https URL](https://github.com/SeunghunLee/SAMDWICH)

## 1 Introduction

Referring Video Object Segmentation (RVOS) is a challenging task focused on identifying and segmenting objects in a video sequence based on a given language description. This task has earned significant attention due to its wide-ranging applications in areas such as video editing and human-robot interaction. Unlike conventional video segmentation tasks, such as Video Instance Segmentation (VIS) (Yang, Fan, and Xu 2019) and Video Object Segmentation (VOS) (Perazzi et al. 2016), RVOS requires a sophisticated cross-modal understanding to accurately localize and track target objects guided by linguistic descriptions. Recent works (Ding et al. 2023; He and Ding 2024) highlight the inherent challenges

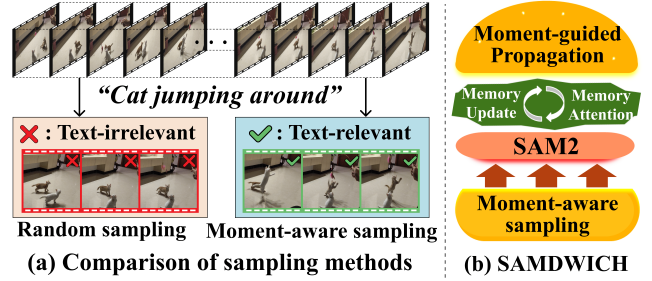


Figure 1: **Importance of moment-aware approach.** (a) Most existing methods rely on random frame sampling, leading to unnatural learning dynamics where models are forced to segment referred objects even in frames unrelated to the given text. (b) We propose a novel RVOS pipeline, SAMDWICH, that explicitly focuses on text-relevant moments to enable semantically grounded segmentation.

of RVOS, especially in dynamically modeling object trajectories to match nuanced language descriptions and complex motion patterns.

With the growing interest in aligning visual and linguistic modalities, recent studies (Wu et al. 2022; Botach, Zheltonozhskii, and Baskin 2022) have explored integrating text prompts with transformer-based segmentation architectures (Zhu et al. 2020; Cheng et al. 2022), leading to notable improvements in cross-modal understanding. Building upon these foundations, several methods enhance temporal modeling of object trajectories (Han et al. 2023; Tang, Zheng, and Yang 2023; Wu et al. 2023; Ding et al. 2023; He and Ding 2024), while others focus on refining the semantic correspondence between language expressions and visual content (Li et al. 2023c; Luo et al. 2024). More recently, the field has begun leveraging large-scale vision foundation models, such as the Segment Anything Model (SAM) (Kirillov et al. 2023; Ravi et al. 2024). Several methods (Yan et al. 2024; Cuttano et al. 2025; Gong et al. 2025; Lin et al. 2025) incorporate SAM to exploit its strong spatial priors and generalization capabilities, achieving impressive results on standard RVOS benchmarks such as Ref-YouTube-VOS (Seo, Lee, and Han 2020) and Ref-DAVIS (Khoreva, Rohrbach, and Schiele 2019). However, these methods struggle on the MeViS benchmark (Ding et al. 2023), largely due to the

\*These authors contribute equally to this work.

lack of explicit guidance for aligning language with semantically relevant visual content. As a result, they often rely on random frame sampling during training, which can include frames unrelated to the expression and weaken vision-language correspondence, as shown in Fig. 1-(a).

To address this, we introduce **MeViS-M**, a new dataset that augments MeViS with manually annotated frame intervals specifying the temporal scope of each expression. These annotations provide explicit supervision signals for aligning language with the most relevant video segments. Building on this dataset, we propose *SAMDWICH*, a novel RVOS framework that improves video-text alignment by focusing supervision on text-relevant moments. *SAMDWICH* incorporates moment-aware supervision, allowing the model to attend to the most informative temporal segments for accurate object grounding. Unlike previous methods that rely on random sampling, *SAMDWICH* leverages semantically aligned supervision to reduce ambiguity and improve consistency. This targeted training strategy enables *SAMDWICH* to achieve robust performance in complex video scenarios with dense object interactions and fine-grained expressions.

Our *SAMDWICH* framework includes *Moment-guided Dual-path Propagation (MDP)*, a simple yet effective strategy that decouples object grounding and tracking. For expression-relevant frames, the model segments referred objects using language-conditioned features, storing the resulting masks and features in a memory bank. For unrelated frames, it propagates these masks using language-agnostic features, thereby avoiding semantic interference. This separation ensures precise grounding where necessary and consistent tracking across the video. In addition, we introduce *Object-level Selective Supervision (OSS)*, a targeted supervision mechanism that selectively assigns ground-truth masks only to objects that are both text-relevant and temporally aligned with the expression, rather than supervising all objects in sampled frames as conventional methods do. By focusing on frames where the referred object is both prominent and semantically grounded in the expression, this approach reduces supervision noise and enhances segmentation accuracy. Extensive experiments demonstrate that *SAMDWICH* outperforms state-of-the-art methods on standard RVOS benchmarks, excelling in challenging video sequences. Our contributions are as follows:

1. We present *SAMDWICH*, a novel RVOS framework that aligns visual content with language through focused supervision on text-relevant moments, utilizing the augmented RVOS dataset.
2. We propose *Moment-guided Dual-path Propagation (MDP)* that ensures temporal consistency by propagating masks from text-relevant frames to others with a moment-centric memory bank.
3. We introduce *Object-level Selective Supervision (OSS)*, which refines supervision by focusing on each object’s relevance to text, strengthening video-text correspondence.
4. We achieve state-of-the-art performance on the challenging MeViS benchmark, setting new standards for text-driven video segmentation.

## 2 Related Works

### 2.1 Referring Video Object Segmentation

Ref-YouTube-VOS (Seo, Lee, and Han 2020) and Ref-DAVIS (Yang, Fan, and Xu 2019) originally defined the core challenges of RVOS, where the goal is to segment objects in videos based on natural language descriptions. With the advent of transformer-based segmentation architectures (Cheng et al. 2022; Zhu et al. 2020), many RVOS methods began to adopt query-driven frameworks to better align visual content with language. MTTR (Botach, Zheltonozhskii, and Baskin 2022) leverages a Video Swin Transformer to model spatio-temporal context, while ReferFormer (Wu et al. 2022) improves grounding through multi-scale feature aggregation and text-conditioned queries. To address the limitations of early benchmarks—such as simple expressions and single-object scenarios—MeViS (Ding et al. 2023) introduces more complex descriptions involving multiple objects per video, along with a motion-aware baseline that enhances temporal modeling. Building on this, He et al. (He and Ding 2024) proposed a method that explicitly decouples static and motion cues, further improving temporal consistency and segmentation accuracy. More recently, the rise of vision-language models (VLMs) has spurred the development of large-scale reasoning-based approaches. VISA (Yan et al. 2024), for example, utilizes Chat-UniVi (Jin et al. 2024) as a video reasoning agent to identify relevant keyframes, segments them using SAM (Kirillov et al. 2023), and propagates masks with XMem (Cheng and Schwing 2022). Several methods (Gong et al. 2025; Lin et al. 2025) follow a similar paradigm, adopting powerful segmentation models like SAM and employing multimodal LLMs such as Chat-UniVi and LLaVA (Liu et al. 2023) as reasoning modules. SAMWISE (Cuttano et al. 2025) introduces a lightweight cross-modal adapter that enables effective text grounding within SAM2 (Ravi et al. 2024). Despite these advances, accurately identifying text-relevant keyframes remains a key bottleneck. This step is critical for robust grounding, especially in complex scenarios requiring temporal consistency and multi-object reasoning.

### 2.2 Vision-Language Models

CLIP (Radford et al. 2021) pioneered large-scale image-text alignment via contrastive pre-training, with extensions (Jia et al. 2021; Li et al. 2021) introducing cross-modal objectives. Caption-augmented methods (Yu et al. 2022; Li et al. 2022) enhance alignment by combining contrastive and captioning objectives. BLIP-2 (Li et al. 2023a) bridges vision encoders and LLMs with a lightweight Query Transformer. In the video domain, Unmasked Teacher (Li et al. 2023b) extends masked modeling to video, LLaMA-Vid (Li, Wang, and Jia 2024) compresses frames for efficiency, and Chat-UniVi (Jin et al. 2024) introduces dynamic multi-scale tokens. Qwen2.5-VL (Bai et al. 2025) employs dynamic resolution and temporal encoding for long videos, while InternVL3 (Zhu et al. 2025) performs a pretraining without LLM adaptation for better multimodal alignment. Despite these advances, achieving consistent fine-grained alignment in complex video scenarios remains challenging.

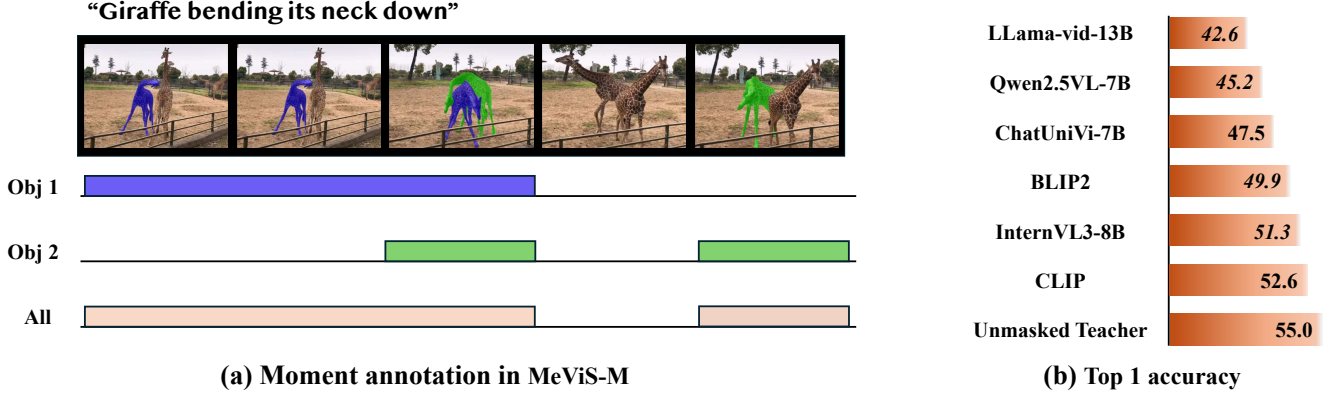


Figure 2: **MeViS-M dataset and analysis on valid.** (a) A moment annotation example from MeViS-M, showing temporal spans labeled for each object referred to by the given expression. (b) Comparison of top-1 accuracy for key frame selection on VLMs. The consistently low accuracy across all models underscores the limitation of existing VLMs in moment retrieval and highlights the necessity of fine-grained moment annotations.

### 3 MeViS-M Dataset

MeViS (Ding et al. 2023) poses a significant challenge for video-text alignment due to its large number of objects and the frequent use of motion-centric expressions. While the dataset offers dense annotations across diverse scenarios, it lacks explicit annotations for text-relevant moments—temporal intervals during which objects perform actions or exhibit states described by the referring sentence. This absence leads existing methods to rely on random frame sampling during training, which often includes frames irrelevant to the expression. Consequently, such indiscriminate sampling hinders effective video-text alignment, making it more difficult for models to associate the referring sentence with the correct object across time.

To address this issue, we introduce **MeViS-M** dataset, an augmented version of the MeViS dataset with explicit moment annotations that enable finer-grained video-text alignment during training. Since a referring sentence may describe specific actions or states involving one or more objects, we annotate text-relevant temporal spans on a per-object basis. For each video, we manually identify the temporal intervals during which each object is semantically relevant to the referring expression, resulting in object-specific moment sets. Formally, for each object  $i$ , we define a moment index set  $\mathcal{M}_i \subseteq \{1, \dots, T_V\}$ , where  $T_V$  is the total number of frames in the video. The union of these sets across all objects constitutes the set of text-relevant moment indices,  $\mathcal{M}^+ = \bigcup_i \mathcal{M}_i$ , while its complement  $\mathcal{M}^- = \{1, \dots, T_V\} \setminus \mathcal{M}^+$  representing irrelevant frames. As an illustrative example shown in Fig. 2-(a), we define  $\mathcal{M}_1 = \{1, 2, 3\}$  and  $\mathcal{M}_2 = \{3, 5\}$ , which results in the text-relevant moment set  $\mathcal{M}^+ = \{1, 2, 3, 5\}$  and its complement  $\mathcal{M}^- = \{4\}$ . These fine-grained annotations allow SANDWICH to focus training specifically on  $\mathcal{M}^+$ , thereby significantly improving both video-text alignment and segmentation performance.

**Analysis.** We evaluate representative VLMs for keyframe

selection on the MeViS-M validation set using the provided moment labels. We measure the top-1 accuracy by checking whether the frame predicted as most relevant to the text is located within the ground-truth moment interval, excluding videos where the ground-truth moment spans the entire video. As shown in Fig. 2-(b), all models exhibit relatively poor performance, with top-1 accuracy hovering around 50%, highlighting the difficulty of accurately identifying text-relevant moments. Recent RVOS approaches (Yan et al. 2024; Gong et al. 2025; Lin et al. 2025) commonly utilize models such as CLIP (Radford et al. 2021), LLaMA-VID (Li, Wang, and Jia 2024), or Chat-UniVi (Jin et al. 2024) for keyframe selection during inference. However, these models are not explicitly trained for fine-grained temporal grounding, often leading to suboptimal or semantically inconsistent keyframe choices. This limitation underscores the importance of a moment-aware approach that can more reliably localize and segment objects based on text-grounded temporal cues.

### 4 SANDWICH

We present *SANDWICH*, a novel RVOS framework designed to improve video-text alignment by explicitly leveraging text-relevant moments, as illustrated in Fig. 3. Given a video  $V = \{I_t\}_{t=1}^{T_V}$  consisting of  $T_V$  frames and a linguistic expression  $E = \{e_l\}_{l=1}^L$  composed of  $L$  words, the objective is to segment and temporally track the objects mentioned in the expression throughout the video. SANDWICH achieves this through the following key components: (1) *Moment-guided Dual-path Propagation (MDP)*, which enables consistent object tracking across both text-relevant and irrelevant frames by learning propagation with a moment-centric memory bank, and (2) *Object-level Selective Supervision (OSS)*, which improves supervision by filtering out objects unrelated to the expression in the sampled clip.



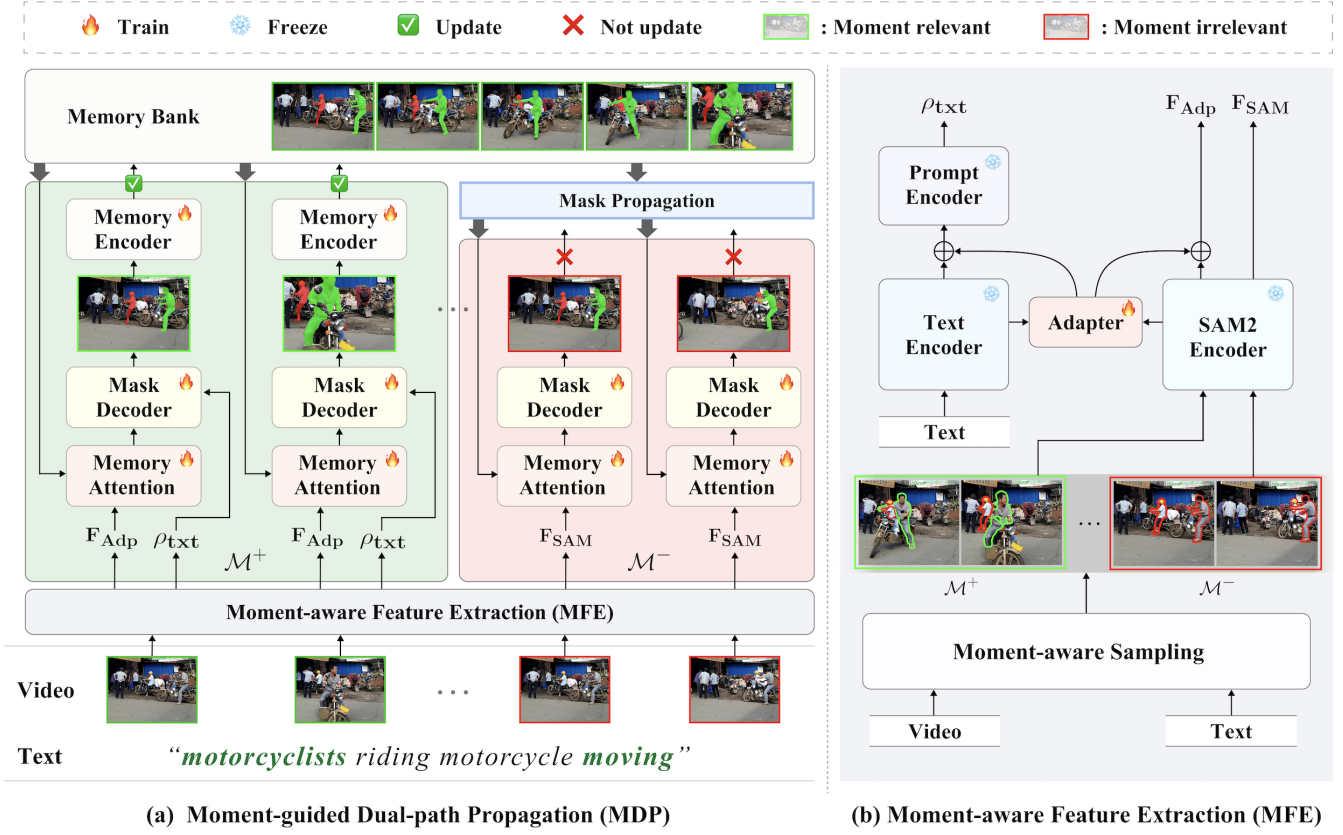


Figure 3: **Overall pipeline.** In (a),  $F_{Adp}$  of text-relevant frames are utilized for mask generation and memory update, while text-irrelevant frames employ  $F_{SAM}$  for mask generation without contributing to the memory update. (b) illustrates how  $F_{Adp}$  and  $F_{SAM}$  are extracted from relevant and irrelevant frames, respectively, and how visual features are integrated into the prompt.

#### 4.1 Baseline Architecture

We adopt SAM2 (Ravi et al. 2024) and RoBERTa (Liu et al. 2019) for video segmentation and text encoding. To enable effective vision-language interaction, we employ a lightweight adapter module (Cuttano et al. 2025), which fuses visual and textual features through bidirectional cross-attention. Given a video  $V = \{I_t\}_{t=1}^{T_V}$  and a referring expression  $E = \{e_l\}_{l=1}^L$ , we sample a short clip consisting of  $T$  frames for training. We extract intermediate visual features  $F^k \in \mathbb{R}^{T \times H_k \times W_k \times C_k}$  from the visual encoder, and textual embeddings  $E^k \in \mathbb{R}^{L \times D}$  from the text encoder at the  $k$ -th layer. The adapter module updates both features via bidirectional cross-attention as follows:

$$\begin{aligned} F_{Adp}^k &= F^k + h(F^k W_{down}^v, E^k W_{down}^t) W_{up}^v, \\ E_{Adp}^k &= E^k + h(E^k W_{down}^t, F^k W_{down}^v) W_{up}^t, \end{aligned} \quad (1)$$

where  $h(\cdot, \cdot)$  denotes a cross-attention function. Here,  $W_{down}^v$  and  $W_{down}^t$  are learnable down-projection matrices for visual and textual features, respectively. Correspondingly,  $W_{up}^v$  and  $W_{up}^t$  are the learnable up-projection matrices. We refer to the outputs of the final (i.e.,  $K$ -th) adapter layer as  $F_{Adp} := F_{Adp}^K$  and  $E_{Adp} := E_{Adp}^K$ .

To construct a text prompt, we leverage the adapter-enhanced text features  $E_{Adp}$ , where  $E_C$  denotes the context-

tual embedding from the [CLS] token, and  $E_M$  represents the motion-centric embedding extracted from verb-related tokens. These embeddings are concatenated via the function  $\psi(\cdot, \cdot)$  and passed through an MLP:

$$\rho_{txt} = \text{MLP}(\psi(E_C, E_M)). \quad (2)$$

We first compute memory-attended visual features  $F_{mem}$  using a memory attention module (Ravi et al. 2024), which attends over the current adaptive feature  $F_{Adp}$  using a memory bank  $\mathcal{B}$ . The resulting feature  $F_{mem}$  is then passed to the mask decoder  $\mathcal{D}$  along with the text prompt  $\rho_{txt}$  to produce soft segmentation mask  $\mathbf{P} \in \mathbb{R}^{H \times W}$ :

$$\mathbf{P} = \mathcal{D}(F_{mem}, \rho_{txt}), \quad F_{mem} = \text{MemoryAttn}(F_{Adp}, \mathcal{B}). \quad (3)$$

The memory bank  $\mathcal{B}$  is updated using the soft mask  $\mathbf{P}$ , following the strategy introduced in SAM2 (Ravi et al. 2024) to enhance temporal consistency. The prompt input  $\rho_{txt}$  is optional and used only when available (e.g., during the initial grounding stage). We obtain the final binary mask via thresholding:  $\hat{\mathbf{Y}} = (\mathbf{P} > 0)$ .

#### 4.2 Design Motivation

A natural strategy for moment-aware RVOS is to train the model solely on text-relevant moments, denoted as  $\mathcal{M}^+$ .



This approach directs the model’s attention toward aligning visual content with the referring expression by providing supervision only on the frames that are semantically consistent with the input text. During inference, the model first performs moment retrieval to identify  $\mathcal{M}^+$ , segments the referred object within these frames, and subsequently propagates the segmentation masks to the remaining, non-relevant frames  $\mathcal{M}^-$ . Although training on the text-relevant frames  $\mathcal{M}^+$  encourages the model to align visual features with the referring expression  $\mathcal{E}$ , this naive strategy introduces two significant challenges at inference time: (1) applying text-conditioned features to semantically irrelevant frames  $\mathcal{M}^-$  can introduce misleading signals, and (2) a mismatch arises between memory features (from  $\mathcal{M}^+$ ) and query features (from  $\mathcal{M}^-$ ), impairing effective mask propagation.

First, conditioning all frames on  $E$  is suboptimal, especially for  $\mathcal{M}^-$ , which lacks visual evidence corresponding to the expression. Applying the adapter to these irrelevant frames may introduce noise or ambiguity. To address this, it is more appropriate to rely on raw visual features  $\mathbf{F}_{\text{SAM}}$ —extracted from the frozen SAM2 encoder—without text conditioning for  $\mathcal{M}^-$ . Second, this asymmetric feature design leads to a feature inconsistency during inference. Specifically, the memory bank is constructed using text-conditioned features  $\mathbf{F}_{\text{Adp}}$  from  $\mathcal{M}^+$ , while memory queries are performed using the unconditioned features  $\mathbf{F}_{\text{SAM}}$  from  $\mathcal{M}^-$ . However, since the model is trained exclusively on  $\mathcal{M}^+$ , it never learns to conduct memory attention using unconditioned query features like  $\mathbf{F}_{\text{SAM}}$ . This discrepancy between memory and query representations degrades the model’s ability to propagate masks accurately, ultimately resulting in poor tracking performance.

### 4.3 Moment-guided Dual-path Propagation

We propose *Moment-guided Dual-path Propagation (MDP)*, a strategy designed to improve both semantic grounding and consistent tracking by selectively leveraging frames within and outside the referred moment. At the core of MDP is a *moment-aware feature extraction (MFE)* strategy that first partitions each video into text-relevant ( $\mathcal{M}^+$ ) and text-irrelevant ( $\mathcal{M}^-$ ) segments using either moment annotations or a retrieval model. By handling  $\mathcal{M}^+$  and  $\mathcal{M}^-$  differently, MDP encourages the model to jointly learn cross-modal alignment and temporal consistency.

For frames in the text-relevant segment  $\mathcal{M}^+$ , we apply a cross-modal adapter to extract text-conditioned features  $\mathbf{F}_{\text{Adp}}$ . In contrast, for frames in the text-irrelevant segment  $\mathcal{M}^-$ , we use the raw visual features  $\mathbf{F}_{\text{SAM}}$  obtained from the frozen SAM2 encoder to prevent semantic contamination from unrelated textual input. To support memory-based reasoning, we compute memory-attended features for both segments using a shared memory attention module and a memory bank  $\mathcal{B}$  as follows:

$$\begin{aligned}\mathbf{F}_{\text{mem}}^+ &= \text{MemoryAttn}(\mathbf{F}_{\text{Adp}}, \mathcal{B}), \\ \mathbf{F}_{\text{mem}}^- &= \text{MemoryAttn}(\mathbf{F}_{\text{SAM}}, \mathcal{B}).\end{aligned}\quad (4)$$

The decoder  $\mathcal{D}$  then predicts the soft segmentation mask  $\mathbf{P}$  by conditioning on the appropriate memory-attended feature. For  $\mathcal{M}^+$ , the decoder also receives the text prompt  $\rho_{\text{txt}}$ ;

for  $\mathcal{M}^-$ , only visual information is used:

$$\mathbf{P} = \begin{cases} \mathcal{D}(\mathbf{F}_{\text{mem}}^+, \rho_{\text{txt}}), & \text{if } t \in \mathcal{M}^+, \\ \mathcal{D}(\mathbf{F}_{\text{mem}}^-), & \text{if } t \in \mathcal{M}^-. \end{cases} \quad (5)$$

This dual-pathway design enables the model to ground the expression precisely within  $\mathcal{M}^+$ , while relying on memory-guided propagation for consistent segmentation across  $\mathcal{M}^-$ .

To enable robust tracking beyond the text-relevant segment  $\mathcal{M}^+$ , we adopt the memory bank management strategy from SAM2 (Ravi et al. 2024), with a key modification: the memory bank stores features exclusively from  $\mathcal{M}^+$ . This design choice ensures that all memory entries used for guidance are semantically grounded by the referring expression. During inference, when processing frames in the text-irrelevant segment  $\mathcal{M}^-$ , the model retrieves memory features from  $\mathcal{M}^+$  to assist segmentation. By attending to these reliable, text-aligned memory representations—rather than relying on local frame-to-frame continuity—the model is better equipped to track objects across ambiguous or visually uninformative regions. This memory-driven mechanism reduces error accumulation and significantly improves the temporal stability and long-range consistency of the segmentation masks.

### 4.4 Object-level Selective Supervision

Conventional RVOS methods supervise the model using ground-truth (GT) masks for all objects visible in the sampled frames, regardless of whether they are semantically relevant to the referring expression. However, in moment-aware scenarios, each object  $i$  is associated with a distinct text-relevant moment  $\mathcal{M}_i$ , which specifies the temporal span during which the object is referred to by the expression  $E$ . Consequently, sampled frames may include objects that are visually present but not semantically aligned with the text query, introducing supervisory noise and weakening cross-modal alignment.

To mitigate this issue, we introduce an object-filtered supervision strategy called *Object-level Selective Supervision (OSS)*, which leverages object-wise moment annotations to selectively supervise only the relevant objects in each training clip. Given a sampled frame index set  $\mathcal{T}$  of length  $T$ , we discard the GT masks of any object  $i$  whose annotated moment  $\mathcal{M}_i$  does not overlap with  $\mathcal{T}$ , i.e., when  $\mathcal{T} \cap \mathcal{M}_i = \emptyset$ . We retain only those masks  $\mathbf{Y}_t^i \in \mathbb{R}^{H \times W}$  for which the condition  $\mathcal{T} \cap \mathcal{M}_i \neq \emptyset$  holds. The resulting filtered set of ground-truth masks is defined as:

$$\mathbf{Y}_{\text{OSS}} = \bigcup_{t \in \mathcal{T}} \{\mathbf{Y}_t^i \mid \mathcal{T} \cap \mathcal{M}_i \neq \emptyset\}. \quad (6)$$

We use this filtered mask set  $\mathbf{Y}_{\text{OSS}}$  to supervise the model’s predictions  $\mathbf{P}_{\mathcal{T}}$  over the sampled frame interval  $\mathcal{T}$ . The final training loss combines the Dice loss  $\mathcal{L}_{\text{Dice}}$  and Focal loss  $\mathcal{L}_{\text{Foc}}$  (Lin et al. 2017) as follows:

$$\mathcal{L} = \lambda_{\text{Dice}} \mathcal{L}_{\text{Dice}}(\mathbf{Y}_{\text{OSS}}, \mathbf{P}_{\mathcal{T}}) + \lambda_{\text{Foc}} \mathcal{L}_{\text{Foc}}(\mathbf{Y}_{\text{OSS}}, \mathbf{P}_{\mathcal{T}}). \quad (7)$$

By aligning supervision targets with the temporal scope of the referring expression, *Object-level Selective Supervision* effectively filters out semantically irrelevant objects, thereby improving the precision of cross-modal learning and enhancing segmentation performance in RVOS.

Method	Visual Encoder	Text Encoder	Total Params	$\mathcal{J}\&\mathcal{F}$	$\mathcal{J}$	$\mathcal{F}$
<b>Large VLM based</b>						
LISA (Lai et al. 2024) [CVPR’24]	ViT-H	LLaVa	7 B	37.2	35.1	39.4
VISA <sup>†</sup> (Yan et al. 2024) [ECCV’24]	ViT-H	Chat-UniVi	7 B	43.5	40.7	46.3
VideoLISA (Bai et al. 2024) [NIPS’24]	ViT-H	Phi-3	3.8 B	42.3	39.4	45.2
VRS-HQ <sup>†</sup> (Gong et al. 2025) [CVPR’25]	Hiera-L	Chat-UniVi	7 B	50.6	47.6	53.7
GLUS <sup>†</sup> (Lin et al. 2025) [CVPR’25]	Hiera-L	LLaVa	7 B	51.3	48.5	54.2
<b>Regular Methods</b>						
MTTR (Botach, Zheltonozhskii, and Baskin 2022) [CVPR’22]	V-Swin-T	RoBERTa	-	30.0	28.8	31.2
ReferFormer (Wu et al. 2022) [CVPR’22]	V-Swin-B	RoBERTa	237 M	31.0	29.8	32.2
OnlineRefer (Wu et al. 2023) [ICCV’23]	Swin-L	RoBERTa	232 M	32.3	31.5	33.1
LMPM (Ding et al. 2023) [ICCV’23]	Swin-T	RoBERTa	195 M	37.2	34.2	40.2
DsHmp (He and Ding 2024) [CVPR’24]	Swin-T	RoBERTa	272 M	46.4	43.0	49.8
SAMWISE (Cuttano et al. 2025) [CVPR’25]	Hiera-B	RoBERTa	202 M	49.5	46.6	52.4
SAMWISE <sup>†</sup> (Cuttano et al. 2025) [CVPR’25]	Hiera-B	RoBERTa	202 M	48.9	46.0	51.7
Ours <sup>†</sup>	Hiera-B	RoBERTa	202 M	<b>51.6</b>	<b>48.8</b>	<b>54.5</b>
<b>Oracle</b>						
SAMWISE (Cuttano et al. 2025) [CVPR’25]	Hiera-B	RoBERTa	202 M	50.3	47.4	53.3
GLUS (Lin et al. 2025) [CVPR’25]	Hiera-L	LLaVa	7B	51.5	48.7	54.3
Ours	Hiera-B	RoBERTa	202 M	53.5	50.7	56.3
Ours	Hiera-L	RoBERTa	355 M	55.1	52.6	57.7
Ours <sup>†</sup>	Hiera-B	RoBERTa	202 M	54.8	52.1	57.5
Ours <sup>†</sup>	Hiera-L	RoBERTa	355 M	<b>55.7</b>	<b>52.9</b>	<b>58.5</b>

Table 1: Comparison on the MeViS dataset. **Oracle** uses ground-truth moments from MeViS-M at inference. <sup>†</sup> indicates methods that leverage vision-language models (VLMs) for keyframe selection. **Oracle** + Ours<sup>†</sup> uses VLMs to extract keyframes from ground-truth moments. We adopt Chrono (Meinardus et al. 2024) and BLIP-2 (Li et al. 2023a) as keyframe selectors.

## 5 Experiments

We evaluate our proposed method on the MeViS dataset (Ding et al. 2023), comparing it against state-of-the-art approaches using the standard  $\mathcal{J}\&\mathcal{F}$  metric. Specifically,  $\mathcal{J}$  denotes the region similarity (Intersection-over-Union) between predicted and ground-truth masks, while  $\mathcal{F}$  measures contour accuracy. In addition to quantitative results, we present an in-depth analysis of our moment-aware design to highlight its contributions. To further demonstrate the generality of our approach, we report zero-shot performance on two widely used benchmarks: Ref-YTVOS (Seo, Lee, and Han 2020) and Ref-DAVIS (Yang, Fan, and Xu 2019).

Our model is built upon SAM2 (Ravi et al. 2024) as the base segmentation framework, with Hiera-Base and Hiera-Large (Ryali et al. 2023) serving as the visual backbones. We use RoBERTa (Liu et al. 2019) as the text encoder. Further details are described in our Supplementary Materials.

### 5.1 Main Results on MeViS

We present the main results on the MeViS dataset in Tab. 1, comparing our method against recent approaches categorized into non-VLM-based (regular) and VLM-based approaches. For a fair comparison, we additionally evaluate the strongest baselines from each category—SAMWISE (non-VLM-based) and GLUS (VLM-based)—under an **Oracle** setting, where ground-truth moment intervals from the MeViS-M dataset are provided at inference time. This setup allows us to analyze the models’ capability to leverage temporally grounded information when it is explicitly available.

We begin by comparing against SAMWISE (Cuttano et al. 2025), the most competitive non-VLM-based method. SAMWISE adopts the same Hiera-B backbone as our model, and the only difference lies in the train-

ing paradigm—ours explicitly models moment-aware alignment, while SAMWISE learns object grounding without temporal localization. Under oracle moment supervision, SAMWISE achieves 50.3  $\mathcal{J}\&\mathcal{F}$ , while our method reaches 53.5, outperforming it by 3.2 points. This performance gap demonstrates that even with identical architectures, explicitly modeling the moment structure leads to significantly better temporal grounding and segmentation.

Next, we evaluate against GLUS (Lin et al. 2025), the strongest VLM-based method, which utilizes a large-scale Hiera-L backbone and is trained on a massive corpus of video-text data. Despite its scale and powerful visual-language pretraining, GLUS achieves only 51.3  $\mathcal{J}\&\mathcal{F}$  under the default setting. When provided with oracle moment intervals, the performance improves marginally to 51.5, indicating limited ability to leverage temporally grounded semantics without explicit temporal modeling. In contrast, our method achieves 55.1  $\mathcal{J}\&\mathcal{F}$  using the same Hiera-L backbone, outperforming GLUS by a large margin of 3.6 points. This result suggests that large-scale pretraining alone is insufficient for precise video-language alignment, and that moment-aware modeling is essential for understanding object-centric temporal structure.

To examine the impact of moment localization, we evaluate our method in a boosted setting incorporating predicted peak moment intervals from the BLIP-2 model (Li et al. 2023a) alongside GT moment annotations. By extracting 8 peak frames and then guiding the model with ground-truth supervision, we achieve improved performance—54.8 with Hiera-B and 55.7 with Hiera-L. This highlights that even coarse moment cues can enhance grounding quality when used to focus supervision, further validating the benefits of a moment-aware formulation for accurate segmentation.

Train with MeViS-M	MDP	OSS	$\mathcal{J}\&\mathcal{F}$
			56.8
✓			58.0
✓	✓		59.4
✓		✓	58.3
✓	✓	✓	<b>60.8</b>

Table 2: Ablation study on main components.

MFE	Memory bank	$\mathcal{J}\&\mathcal{F}$
	All frames	58.0
	$\mathcal{M}^+$	58.9
✓	All frames	60.3
✓	$\mathcal{M}^+$	<b>60.8</b>

Table 3: Ablation study on MDP. Note that when MFE is not used,  $F_{\text{adp}}$  is applied even within the  $\mathcal{M}^-$  interval.

## 5.2 Further Analysis

All experiments in this section are conducted using the Hiera-B backbone, and the results are reported in terms of  $\mathcal{J}\&\mathcal{F}$  score on the valid\_u set of MeViS-M dataset.

**Ablation study on main components.** Our method integrates three core components: moment-aware sampling based on MeViS-M, Moment-guided Dual-path Propagation (MDP), and Object-level Selective Supervision (OSS). As shown in Tab. 2, training without any moment-aware design yields a score of 56.8. Incorporating moment-aware sampling via MeViS-M provides a modest improvement to 58.0. Adding either MDP or OSS individually yields further gains, reaching 59.4 and 58.3, respectively. When all components are combined, our model achieves 60.8, confirming that each contributes complementarily to the final performance. Notably, this represents a significant improvement of **+4.0 points** over the baseline, highlighting the effectiveness of our moment-aware formulation.

**Ablation study on MDP.** Tab. 3 analyzes two core design elements within MDP: (1) Moment-aware Feature Enhancement (MFE), and (2) selective memory construction using only  $\mathcal{M}^+$  frames. Without MFE and using a memory bank built from all frames, the model achieves 58.0. Restricting the memory bank to  $\mathcal{M}^+$  improves the performance to 58.9. Applying alone yields a larger gain of 60.3, and combining both MFE and selective memory results in the highest score of 60.8. These results validate that both components are critical to achieving accurate propagation.

**Comparison of sampling methods.** Tab. 4 compares three sampling methods: random sampling, BLIP-2, and MeViS-M. For BLIP-2-based sampling, we select the frame predicted as most relevant to the given text and sample 8 surrounding frames. As analyzed in Fig. 2-(b), BLIP-2 suffers from poor video-text alignment, leading to performance that is 1.3 points lower than random sampling. In contrast,

Method	Random	BLIP-2	MeViS-M
$\mathcal{J}\&\mathcal{F}$	56.8	55.5	58.0

Table 4: Comparison of sampling methods.

Model	Backbone	Ref-YouTube-VOS	Ref-DAVIS
DsHmp	Swin-T	45.8	64.7
SAMWISE	Hiera-B	56.1	65.4
Ours	Hiera-B	<b>60.3</b>	<b>67.4</b>

Table 5: Comparison of zero-shot performance.

MeViS-M provides accurate ground-truth moment intervals, resulting in a performance gain of 1.2 over random sampling and 2.5 over BLIP-2. These results highlight the importance of temporal grounding for accurate video-text alignment.

**Generalization to other datasets.** We also evaluate the generalization ability of our model trained on the MeViS dataset by testing its zero-shot performance on the validation set of two other RVOS benchmarks: Ref-YouTube-VOS (Seo, Lee, and Han 2020) and Ref-DAVIS (Khoreva, Rohrbach, and Schiele 2019). As shown in Tab. 5, our method achieves strong zero-shot results, outperforming recent state-of-the-art approaches such as DsHmp (He and Ding 2024) and SAMWISE (Cuttano et al. 2025) by a notable margin. In particular, our model surpasses DsHmp by +14.5 on Ref-YouTube-VOS and +2.7 on Ref-DAVIS, and outperforms SAMWISE by +4.2 and +2.0 on the respective benchmarks. This highlights the effectiveness of moment-aware training in capturing generalized language-visual alignment across diverse domains.

## 6 Conclusion

We present SANDWICH, a novel moment-aware pipeline for Referring Video Object Segmentation, built on the newly proposed MeViS-M dataset, the first benchmark with explicit object-wise temporal annotations indicating when objects are referred to by language. This dataset enables a better understanding and utilization of temporal dynamics in language grounding for videos. To fully leverage this information, we introduce two complementary methods: Moment-guided Dual-path Propagation, which separates text-relevant and irrelevant frames to improve both semantic grounding and object tracking; and Object-level Selective Supervision, which selectively supervises only the objects relevant to the referred moments. These strategies explicitly model temporal moments, resulting in significant improvements in grounding accuracy and tracking consistency. Extensive experiments on challenging RVOS benchmarks demonstrate that our approach consistently outperforms prior methods, especially in complex scenarios involving multiple objects and temporally sparse language references. These results highlight the crucial importance of moment-aware designs in enhancing video-language understanding and suggest promising directions for future research in temporally grounded video segmentation.



**Acknowledgments** This work was supported by the Ministry of Trade, Industry and Energy (MOTIE), South Korea, through the Technology Innovation Program under Grant RS-2024-00445759, for the development of navigation technology utilizing visual information based on vision-language models for understanding dynamic environments in nonlearned spaces), the National Research Foundation of Korea (NRF) grant funded by the Korea government (MSIT) (No. RS-2023-00210908) and the Institute of Information & Communications Technology Planning & Evaluation (IITP) grant funded by the Korea government (MSIT) (No. RS-2025-02219277, AI Star Fellowship Support Project (DGIST)).

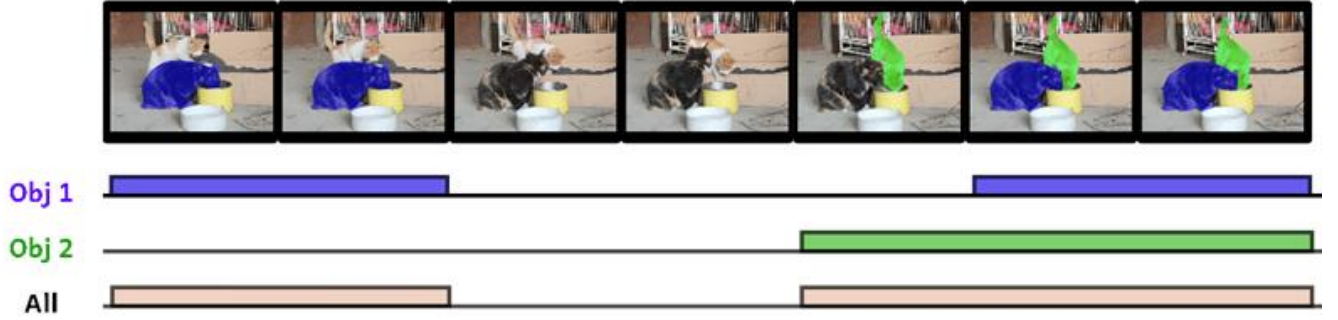
## References

- Bai, S.; Chen, K.; Liu, X.; Wang, J.; Ge, W.; Song, S.; Dang, K.; Wang, P.; Wang, S.; Tang, J.; et al. 2025. Qwen2. 5-vl technical report. *arXiv preprint arXiv:2502.13923*.
- Bai, Z.; He, T.; Mei, H.; Wang, P.; Gao, Z.; Chen, J.; Zhang, Z.; and Shou, M. Z. 2024. One token to seg them all: Language instructed reasoning segmentation in videos. *Advances in Neural Information Processing Systems*, 37: 6833–6859.
- Botach, A.; Zheltonozhskii, E.; and Baskin, C. 2022. End-to-end referring video object segmentation with multimodal transformers. In *Proceedings of the IEEE/CVF Conference on Computer Vision and Pattern Recognition*, 4985–4995.
- Cheng, B.; Misra, I.; Schwing, A. G.; Kirillov, A.; and Girdhar, R. 2022. Masked-attention mask transformer for universal image segmentation. In *Proceedings of the IEEE/CVF conference on computer vision and pattern recognition*, 1290–1299.
- Cheng, H. K.; and Schwing, A. G. 2022. Xmem: Long-term video object segmentation with an atkinson-shiffrin memory model. In *European conference on computer vision*, 640–658. Springer.
- Chung, H. W.; Hou, L.; Longpre, S.; Zoph, B.; Tay, Y.; Fedus, W.; Li, Y.; Wang, X.; Dehghani, M.; Brahma, S.; et al. 2024. Scaling instruction-finetuned language models. *Journal of Machine Learning Research*, 25(70): 1–53.
- Cuttano, C.; Trivigno, G.; Rosi, G.; Masone, C.; and Averta, G. 2025. Samwise: Infusing wisdom in sam2 for text-driven video segmentation. In *Proceedings of the Computer Vision and Pattern Recognition Conference*, 3395–3405.
- Ding, H.; Liu, C.; He, S.; Jiang, X.; and Loy, C. C. 2023. MeViS: A large-scale benchmark for video segmentation with motion expressions. In *Proceedings of the IEEE/CVF International Conference on Computer Vision*, 2694–2703.
- Fang, Y.; Wang, W.; Xie, B.; Sun, Q.; Wu, L.; Wang, X.; Huang, T.; Wang, X.; and Cao, Y. 2023. Eva: Exploring the limits of masked visual representation learning at scale. In *Proceedings of the IEEE/CVF conference on computer vision and pattern recognition*, 19358–19369.
- Gao, J.; Sun, C.; Yang, Z.; and Nevatia, R. 2017. Tall: Temporal activity localization via language query. In *Proceedings of the IEEE international conference on computer vision*, 5267–5275.
- Gong, S.; Zhuge, Y.; Zhang, L.; Yang, Z.; Zhang, P.; and Lu, H. 2025. The Devil is in Temporal Token: High Quality Video Reasoning Segmentation. *arXiv preprint arXiv:2501.08549*.
- Han, M.; Wang, Y.; Li, Z.; Yao, L.; Chang, X.; and Qiao, Y. 2023. Htm: Hybrid temporal-scale multimodal learning framework for referring video object segmentation. In *Proceedings of the IEEE/CVF International Conference on Computer Vision*, 13414–13423.
- He, S.; and Ding, H. 2024. Decoupling static and hierarchical motion perception for referring video segmentation. In *Proceedings of the IEEE/CVF Conference on Computer Vision and Pattern Recognition*, 13332–13341.
- Jia, C.; Yang, Y.; Xia, Y.; Chen, Y.-T.; Parekh, Z.; Pham, H.; Le, Q.; Sung, Y.-H.; Li, Z.; and Duerig, T. 2021. Scaling up visual and vision-language representation learning with noisy text supervision. In *International conference on machine learning*, 4904–4916. PMLR.
- Jin, P.; Takanobu, R.; Zhang, W.; Cao, X.; and Yuan, L. 2024. Chat-univi: Unified visual representation empowers large language models with image and video understanding. In *Proceedings of the IEEE/CVF Conference on Computer Vision and Pattern Recognition*, 13700–13710.
- Khoreva, A.; Rohrbach, A.; and Schiele, B. 2019. Video object segmentation with language referring expressions. In *Computer Vision—ACCV 2018: 14th Asian Conference on Computer Vision, Perth, Australia, December 2–6, 2018, Revised Selected Papers, Part IV 14*, 123–141. Springer.
- Kirillov, A.; Mintun, E.; Ravi, N.; Mao, H.; Rolland, C.; Gustafson, L.; Xiao, T.; Whitehead, S.; Berg, A. C.; Lo, W.-Y.; et al. 2023. Segment anything. In *Proceedings of the IEEE/CVF international conference on computer vision*, 4015–4026.
- Lai, X.; Tian, Z.; Chen, Y.; Li, Y.; Yuan, Y.; Liu, S.; and Jia, J. 2024. Lisa: Reasoning segmentation via large language model. In *Proceedings of the IEEE/CVF Conference on Computer Vision and Pattern Recognition*, 9579–9589.
- Lei, J.; Berg, T. L.; and Bansal, M. 2021. Detecting moments and highlights in videos via natural language queries. *Advances in Neural Information Processing Systems*, 34: 11846–11858.
- Li, J.; Li, D.; Savarese, S.; and Hoi, S. 2023a. Blip-2: Bootstrapping language-image pre-training with frozen image encoders and large language models. In *International conference on machine learning*, 19730–19742. PMLR.
- Li, J.; Li, D.; Xiong, C.; and Hoi, S. 2022. Blip: Bootstrapping language-image pre-training for unified vision-language understanding and generation. In *International conference on machine learning*, 12888–12900. PMLR.
- Li, J.; Selvaraju, R.; Gotmare, A.; Joty, S.; Xiong, C.; and Hoi, S. C. H. 2021. Align before fuse: Vision and language representation learning with momentum distillation. *Advances in neural information processing systems*, 34: 9694–9705.
- Li, K.; Wang, Y.; Li, Y.; Wang, Y.; He, Y.; Wang, L.; and Qiao, Y. 2023b. Unmasked teacher: Towards training-efficient video foundation models. In *Proceedings of the*

- IEEE/CVF International Conference on Computer Vision*, 19948–19960.
- Li, X.; Wang, J.; Xu, X.; Li, X.; Raj, B.; and Lu, Y. 2023c. Robust referring video object segmentation with cyclic structural consensus. In *Proceedings of the IEEE/CVF International Conference on Computer Vision*, 22236–22245.
- Li, Y.; Wang, C.; and Jia, J. 2024. Llama-vid: An image is worth 2 tokens in large language models. In *European Conference on Computer Vision*, 323–340. Springer.
- Lin, L.; Yu, X.; Pang, Z.; and Wang, Y.-X. 2025. GLUS: Global-Local Reasoning Unified into A Single Large Language Model for Video Segmentation. In *Proceedings of the IEEE/CVF Conference on Computer Vision and Pattern Recognition*.
- Lin, T.-Y.; Goyal, P.; Girshick, R.; He, K.; and Dollár, P. 2017. Focal loss for dense object detection. In *Proceedings of the IEEE international conference on computer vision*, 2980–2988.
- Liu, H.; Li, C.; Wu, Q.; and Lee, Y. J. 2023. Visual instruction tuning. *Advances in neural information processing systems*, 36: 34892–34916.
- Liu, Y.; Ott, M.; Goyal, N.; Du, J.; Joshi, M.; Chen, D.; Levy, O.; Lewis, M.; Zettlemoyer, L.; and Stoyanov, V. 2019. Roberta: A robustly optimized bert pretraining approach. *arXiv preprint arXiv:1907.11692*.
- Luo, Z.; Xiao, Y.; Liu, Y.; Li, S.; Wang, Y.; Tang, Y.; Li, X.; and Yang, Y. 2024. Soc: Semantic-assisted object cluster for referring video object segmentation. *Advances in Neural Information Processing Systems*, 36.
- Meinardus, B.; Batra, A.; Rohrbach, A.; and Rohrbach, M. 2024. The surprising effectiveness of multimodal large language models for video moment retrieval. *arXiv preprint arXiv:2406.18113*.
- Nagaraja, V. K.; Morariu, V. I.; and Davis, L. S. 2016. Modeling context between objects for referring expression understanding. In *Computer Vision–ECCV 2016: 14th European Conference, Amsterdam, The Netherlands, October 11–14, 2016, Proceedings, Part IV 14*, 792–807. Springer.
- Perazzi, F.; Pont-Tuset, J.; McWilliams, B.; Van Gool, L.; Gross, M.; and Sorkine-Hornung, A. 2016. A benchmark dataset and evaluation methodology for video object segmentation. In *Proceedings of the IEEE conference on computer vision and pattern recognition*, 724–732.
- Pont-Tuset, J.; Perazzi, F.; Caelles, S.; Arbeláez, P.; Sorkine-Hornung, A.; and Van Gool, L. 2017. The 2017 davis challenge on video object segmentation. *arXiv preprint arXiv:1704.00675*.
- Radford, A.; Kim, J. W.; Hallacy, C.; Ramesh, A.; Goh, G.; Agarwal, S.; Sastry, G.; Askell, A.; Mishkin, P.; Clark, J.; et al. 2021. Learning transferable visual models from natural language supervision. In *International conference on machine learning*, 8748–8763. PmLR.
- Ravi, N.; Gabeur, V.; Hu, Y.-T.; Hu, R.; Ryali, C.; Ma, T.; Khedr, H.; Rädle, R.; Rolland, C.; Gustafson, L.; et al. 2024. Sam 2: Segment anything in images and videos. *arXiv preprint arXiv:2408.00714*.
- Ryali, C.; Hu, Y.-T.; Bolya, D.; Wei, C.; Fan, H.; Huang, P.-Y.; Aggarwal, V.; Chowdhury, A.; Poursaeed, O.; Hoffman, J.; Malik, J.; Li, Y.; and Feichtenhofer, C. 2023. Hiera: A Hierarchical Vision Transformer without the Bells-and-Whistles. *ICML*.
- Seo, S.; Lee, J.-Y.; and Han, B. 2020. Urvos: Unified referring video object segmentation network with a large-scale benchmark. In *Computer Vision–ECCV 2020: 16th European Conference, Glasgow, UK, August 23–28, 2020, Proceedings, Part XV 16*, 208–223. Springer.
- Tang, J.; Zheng, G.; and Yang, S. 2023. Temporal collection and distribution for referring video object segmentation. In *Proceedings of the IEEE/CVF International Conference on Computer Vision*, 15466–15476.
- Wu, D.; Wang, T.; Zhang, Y.; Zhang, X.; and Shen, J. 2023. Onlinerefer: A simple online baseline for referring video object segmentation. In *Proceedings of the IEEE/CVF International Conference on Computer Vision*, 2761–2770.
- Wu, J.; Jiang, Y.; Sun, P.; Yuan, Z.; and Luo, P. 2022. Language as queries for referring video object segmentation. In *Proceedings of the IEEE/CVF Conference on Computer Vision and Pattern Recognition*, 4974–4984.
- Yan, C.; Wang, H.; Yan, S.; Jiang, X.; Hu, Y.; Kang, G.; Xie, W.; and Gavves, E. 2024. Visa: Reasoning video object segmentation via large language models. *arXiv preprint arXiv:2407.11325*.
- Yang, L.; Fan, Y.; and Xu, N. 2019. Video instance segmentation. In *Proceedings of the IEEE/CVF international conference on computer vision*, 5188–5197.
- Yu, J.; Wang, Z.; Vasudevan, V.; Yeung, L.; Seyedhosseini, M.; and Wu, Y. 2022. Coca: Contrastive captioners are image-text foundation models. *arXiv preprint arXiv:2205.01917*.
- Yu, L.; Poirson, P.; Yang, S.; Berg, A. C.; and Berg, T. L. 2016. Modeling context in referring expressions. In *Computer Vision–ECCV 2016: 14th European Conference, Amsterdam, The Netherlands, October 11–14, 2016, Proceedings, Part II 14*, 69–85. Springer.
- Zhu, J.; Wang, W.; Chen, Z.; Liu, Z.; Ye, S.; Gu, L.; Tian, H.; Duan, Y.; Su, W.; Shao, J.; et al. 2025. Internv13: Exploring advanced training and test-time recipes for open-source multimodal models. *arXiv preprint arXiv:2504.10479*.
- Zhu, X.; Su, W.; Lu, L.; Li, B.; Wang, X.; and Dai, J. 2020. Deformable detr: Deformable transformers for end-to-end object detection. *arXiv preprint arXiv:2010.04159*.

## A Appendix

### “Cat eat in a bowl”



### “The two cats that tumbled down from the sofa”

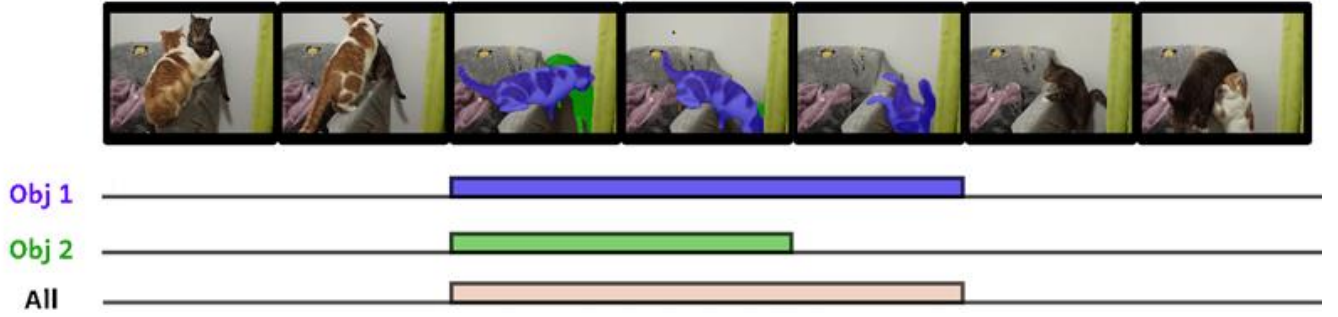


Figure 4: Moment annotataion examples of MeViS-M.

#### A.1 Moment Label Collection

To construct the MeViS-M dataset, we manually annotate text-relevant temporal segments on top of the existing MeViS dataset (Ding et al. 2023), which consists of three splits: *train* (1,662 videos), *valid<sub>u</sub>* (50 videos), and *valid* (140 videos). Since the *valid* split lacks mask ground-truths, we annotate expression-relevant frames only at the video level, rather than assigning object-specific moment spans. In contrast, for *train* and *valid<sub>u</sub>*, we provide detailed moment annotations for each referred object, as shown in Fig. 4.

The annotation process is carried out by approximately 20 annotators, who manually inspect and label each video. During this process, we remove any training samples where the referred objects do not have valid mask annotations, resulting in the removal of 66 videos and 1,278 expressions from the training set. We also make several corrections to the original labels, including adding missing objects that are described in the text but absent from the annotations, and fixing cases of label ID switching. Examples of such corrections are illustrated in Fig. 5, categorized by case type. Fig. 5-(a) involves partial segmentation where the target object is incompletely annotated, and moreover, the MeViS dataset lacks suitable masks to correct the ground truth; therefore, this case was excluded from the dataset. Fig. 5-

(b) involves a frame in which the mask IDs of two turtles are mistakenly swapped, necessitating correction of the ID assignment. Fig. 5-(c) refers to instances where multiple elephants matching the referring expression are present, but only a subset are labeled in the ground-truth; thus, the missing objects are added to the annotations. Conversely, Fig. 5-(d) describes situations where objects not corresponding to the expression are annotated, and these irrelevant masks are subsequently removed. Finally, Fig. 5-(e) combines the issues from Fig. 5-(c) and Fig. 5-(d), resulting in comprehensive corrections across the affected frames. Note that the results reported in the first row of Tab. 2-(a) in the main text (56.8  $\mathcal{J}\&\mathcal{F}$ , without MeViS-M) are also obtained using the corrected labels, except that the moment labels from MeViS-M are not utilized.

#### A.2 Analysis of Moment-aware Inference

In this section, we investigate how the performance of our SANDWICH model, trained using a moment-aware strategy, varies depending on the quality of the moment segments provided at inference time. All evaluations are conducted using the Hiera-Base backbone on the *valid<sub>u</sub>* and *valid* splits of the MeViS-M dataset. Specifically, we compare the model’s  $\mathcal{J}\&\mathcal{F}$  scores under four different condi-



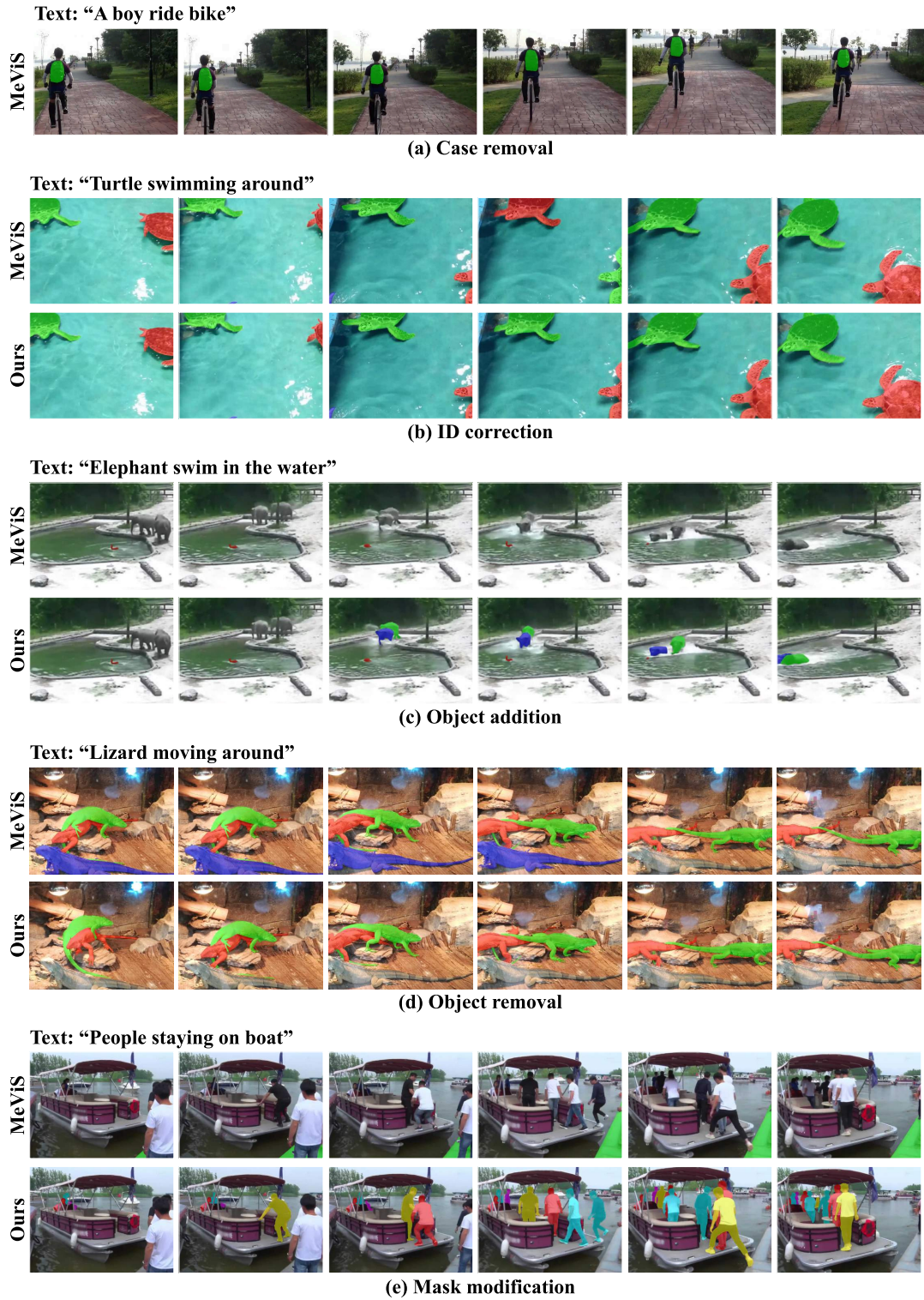


Figure 5: Examples of GT refinement in MeViS-M compared with MeViS.

tions: (1) moment segments using vision-language models (VLMs), (2) segments retrieved by a dedicated moment retrieval model, (3) segments derived by combining outputs from both the VLMs and the retrieval model, and (4) ground-truth moment segments. This analysis underscores the crit-

ical role of accurate moment selection in moment-aware RVOS.

**Inference with VLMs** As shown in Fig. 6-(a), we evaluate our model using moment guidance derived from standard

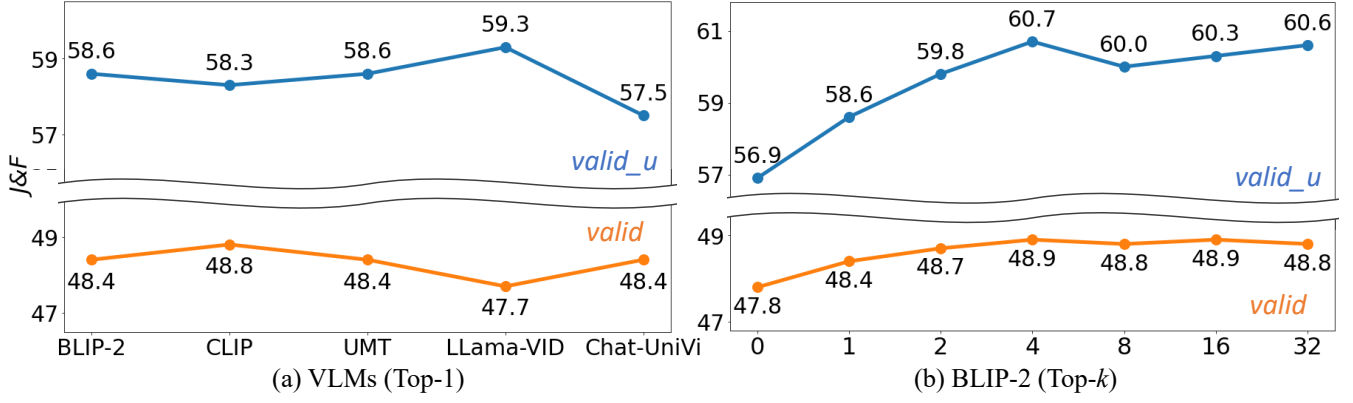


Figure 6: Performance comparison of VLM-based keyframe selection.

Split	R1@.5	R1@.7	mAP	mAP@.5	mAP@.75	$\mathcal{J}\&\mathcal{F}$
$valid\_u$	74.7	61.8	62.1	72.8	60.0	57.6
$valid$	61.3	53.0	52.2	60.6	51.2	50.4

Table 6: Moment retrieval performance.

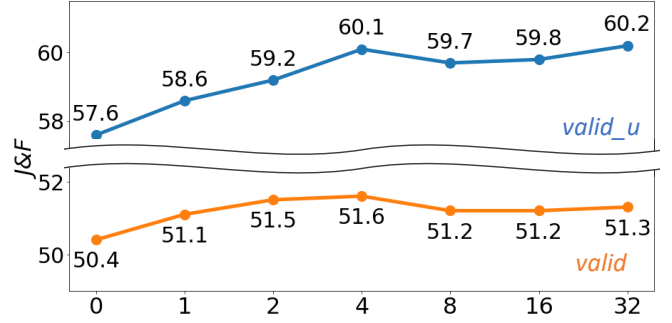


Figure 7: Performance of combining method (Chrono and BLIP-2).

VLMs by selecting the most relevant frame to the given text expression. We compare five representative models: BLIP-2 (Li et al. 2023a), CLIP (Radford et al. 2021), Unmasked Teacher (UMT) (Li et al. 2023b), LLaMA-VID (Li, Wang, and Jia 2024), and Chat-UniVi (Jin et al. 2024). As discussed in Fig. 2 of the main manuscript, the top-1 accuracy on the  $valid$  split is significantly low, which leads to all models showing  $\mathcal{J}\&\mathcal{F}$  scores below 50 on  $valid$ .

Fig. 6-(b) further analyzes the performance of the BLIP-2 model, which achieves the best balance across the two splits. We report performance as we vary the number of top- $k$  selected frames. When using the top-4 frames, our model achieves 60.7 on  $valid\_u$  and 48.9 on  $valid$ , which is the best among all  $k$  values tested. However, this is still more than 4 points lower than the score achieved using ground-truth (GT) moment guidance (53.5 on  $valid$ ), highlighting the limitations of relying solely on VLM-based frame selection.

**Inference with Moment Retrieval Model** Due to the limited video-text alignment capabilities of standard VLMs, we employ Chrono (Meinardus et al. 2024), a state-of-the-art moment retrieval model, to predict relevant temporal segments. As shown in Tab. 6, Chrono achieves an R1@.7 score of 61.8 and mAP of 62.1 on the  $valid\_u$  and R1@.7 score of 53.0 and mAP of 52.2 on the  $valid$ , respectively. Using Chrono’s predicted moments for inference, our model at-

tains a  $\mathcal{J}\&\mathcal{F}$  score of 57.6 on  $valid\_u$  and 50.4 on  $valid$ . These results highlight the importance of accurate moment localization for achieving effective moment-aware video-text alignment in RVOS.

#### Inference with Both VLMs and Moment Retrieval Model

Fig. 7 illustrates the performance when combining VLMs with the moment retrieval model. Specifically, we select the top- $k$  frames with the highest text-relevance scores from BLIP-2 within the temporal segment predicted by Chrono, and prioritize these  $k$  frames during inference. This combined strategy consistently outperforms using Chrono alone. The best performance is observed when using the top-4 frames, achieving  $\mathcal{J}\&\mathcal{F}$  scores of 60.1 on  $valid\_u$  and 51.6 on  $valid$ . These results suggest that prioritizing frames that are highly relevant to the expression—rather than processing the moment segment in temporal order—facilitates more effective localization of the referred object. This finding provides new insights into how aligning textual relevance within retrieved temporal windows can enhance moment-aware RVOS. As shown in Tab. 7, even without using ground-truth moment labels during inference, our method surpasses SAMWISE by 2.1 points on the  $valid$  split, confirming the advantage of our moment-guided strategy.

**Inference with Ground-Truth Moments** In the ideal setting where ground-truth (GT) moments are provided, the

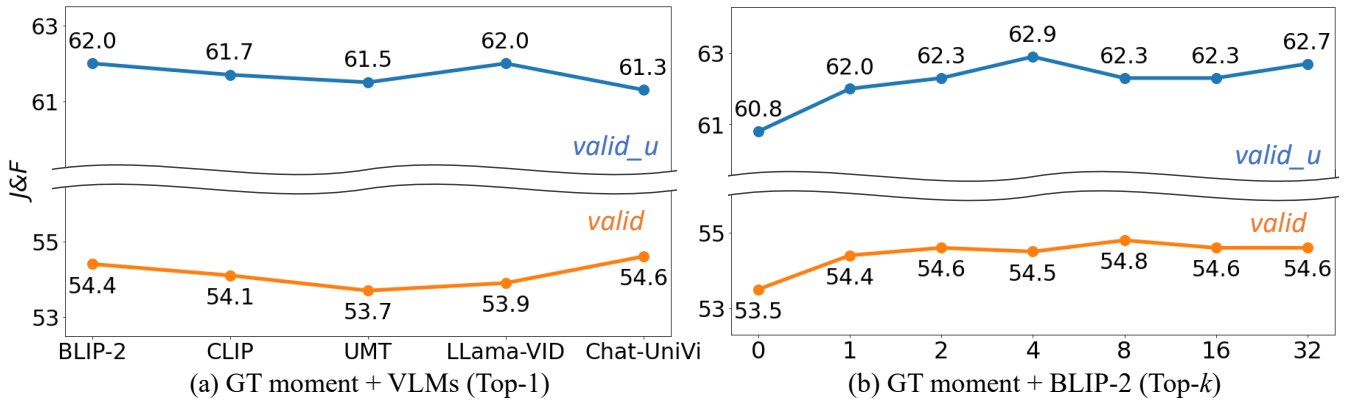


Figure 8: Performance of GT moment segment and VLM-based keyframe selection.

Method	$\mathcal{J}\&\mathcal{F}$
<b>Regular Methods</b>	
SAMWISE (Cuttano et al. 2025)	49.5
Ours	<b>51.6</b>

Table 7: Performance without GT moments.

model achieves notably high  $\mathcal{J}\&\mathcal{F}$  scores of 60.8 on *valid\_u* and 53.5 on *valid*. Furthermore, we examine the impact of prioritizing  $k$  frames with the highest text-relevance scores predicted by BLIP-2 within the GT moment segment, as shown in Fig. 8. This strategy yields consistently strong performance (Fig. 8-(a)), particularly achieving 62.9 on *valid\_u* and 54.5 on *valid* when using the top-4 frames (Fig. 8-(b)). The highest score on *valid*, 54.8, is observed when using the top-8 frames. These results demonstrate the benefit of leveraging textual relevance even within an oracle temporal segment.

**Comparison of Key Frame Selection Methods** Fig. 9 illustrates the Top1 predictions of various key frame selection methods alongside the MeViS-M annotations. In the first and second examples, some VLM models predict a moment that closely matches the annotated interval, demonstrating promising performance for relatively straightforward queries. However, in the third example, the predictions from VLM models are widely scattered across the timeline, failing to localize the annotated moment accurately. This highlights the limitations of current methods in achieving precise temporal localization, especially for complex or ambiguous queries, and demonstrates the need for improved text-video alignment in future models.

### A.3 Implementation Details

**Dataset.** We train our model using moment guidance from the MeViS-M dataset, which consists of 27,292 motion-focused expressions across 1,596, 50, and 140 videos in the *train*, *valid\_u*, and *valid* split, respectively. For evaluation, we test on both the *valid\_u* and *valid* splits of MeViS-M. Additionally, we assess the generalization capability of our

model in a zero-shot setting on two external benchmarks, including Ref-YouTube-VOS (Seo, Lee, and Han 2020) and Ref-DAVIS17 (Khoreva, Rohrbach, and Schiele 2019). Ref-YouTube-VOS augments the original YouTube-VOS dataset (Seo, Lee, and Han 2020) with approximately 15K referring expressions over 3,978 videos, and is split into 3,471 videos for training, 202 for validation, and 305 for testing. Ref-DAVIS17 extends the DAVIS17 (Pont-Tuset et al. 2017) dataset with 1.5K referring expressions annotated across 90 videos (60 for training and 30 for testing), and features high-resolution masks and complex multi-object scenarios.

**RVOS Model.** Our model is built upon SAM2 (Ravi et al. 2024) as the video segmentation framework, with Hiera-Base and Hiera-Large (Ryali et al. 2023) used as visual backbones. For text encoding, we use RoBERTa (Liu et al. 2019), keeping both the image and text encoders frozen during training. Only the cross-modal adapter, mask decoder, and memory modules are updated, resulting in approximately 17M trainable parameters—accounting for just 8.4% of the total parameters. We utilize features from the last three stages of both encoders for the cross-modal adapter module. We sample 8 frames per video for Hiera-Base and 6 frames for Hiera-Large. To ensure temporal consistency, half of the frames are always sampled from the text-relevant segment ( $\mathcal{M}^+$ ), while the other half are drawn from either  $\mathcal{M}^+$  or irrelevant segments ( $\mathcal{M}^-$ ). Following prior works (Wu et al. 2022; Han et al. 2023; Wu et al. 2023; Luo et al. 2024; Cuttano et al. 2025), we pretrain the model on RefCO-CO+/g (Nagaraja, Morariu, and Davis 2016; Yu et al. 2016) for 6 epochs. Final training is conducted on MeViS-M for 1 epoch with a batch size of 4, using the Adam optimizer and a learning rate of  $1 \times 10^{-5}$ . Only features from the  $\mathcal{M}^+$  segment are stored in the memory bank. When performing memory attention, the model attends to features from the 6 nearest frames within the memory. All experiments are conducted on 4 NVIDIA A100 GPUs with 40GB of memory.

**VLMs.** For inference, previous works (Yan et al. 2024; Lin et al. 2025) exploit keyframe selection using VLMs (Li, Wang, and Jia 2024; Jin et al. 2024). For our experiments, we evaluate five VLMs: BLIP-2 (Li et al. 2023a), CLIP (Radford et al. 2021), Unmasked Teacher (UMT) (Li et al.



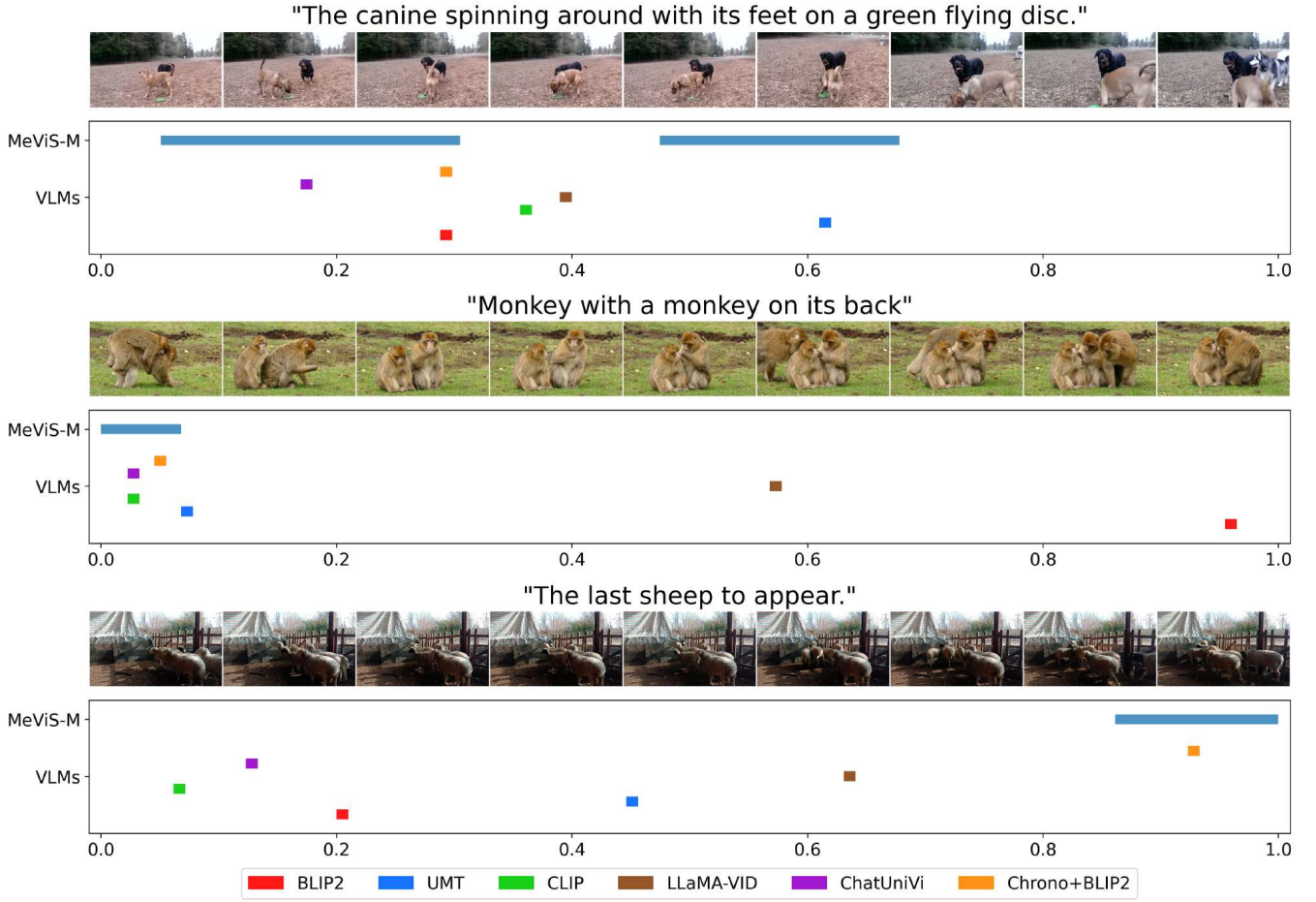


Figure 9: Visualization of key frame selection methods with Top-1 prediction.

2023b), LLaMa-VID (Li, Wang, and Jia 2024), and ChatUniVi (Jin et al. 2024). For BLIP-2, we use a ViT-G (Fang et al. 2023) backbone. For CLIP, we use a ViT-L/14x336 backbone. For UMT, we use a ViT-L/14 backbone pretrained on 25 million image/video-text pairs. For these three models, we compute frame-wise text similarity and select the top- $k$  frames. For LLaMa-VID and ChatUniVi, we use the same keyframe selection method as in (Yan et al. 2024; Lin et al. 2025). Additionally, in Fig. 2 of the main text, we compare the top-1 performance of VLMS on *valid* split, excluding cases where the ground-truth moment spans 100% of the video.

**Moment Retrieval Model.** We employ Chrono (Meinardus et al. 2024) model for moment retrieval, which uses a BLIP-2 backbone with ViT-G (Fang et al. 2023) as the vision encoder and T5-XL (Chung et al. 2024) as the text encoder. For fine-tuning, we upsample MeViS-M samples by a factor of three when their ground-truth moments cover less than 90% of frames, excluding those spanning 90–100%. Detailed hyperparameters follow the Charades-STA (Gao et al. 2017) dataset configuration, with uniform sampling of 40 frames per video during training and 60 frames during inference. We initialize the model with pretrained weights of QVHigh-

lights dataset (Lei, Berg, and Bansal 2021) and finetune for five epochs on four NVIDIA A100 GPUs, with a batch size of one per GPU and gradient accumulation over eight iterations.

#### A.4 Additional Results

**Feature Visualizations** Fig. 10 presents a comparative analysis of feature maps produced by the SAMWISE and SANDWICH models, with visualizations obtained using PCA for dimensionality reduction. The feature representation produced by SAMWISE lacks clear localization and fails to form distinct activations corresponding to the target object described in the expression. This indicates that the model struggles to align regions with the referring text, due to the absence of moment-aware understanding and fine-grained object-level supervision. In contrast, SANDWICH exhibits more focused and semantically meaningful features that accurately highlight the referred object (i.e., dark regions in the **feature maps** of Fig. 10), demonstrating successful visual-text alignment. We attribute this improvement to our moment-aware strategy (MDP) and the use of object-level selective supervision (OSS), which jointly guide the model to identify the most relevant frames and learn dis-

*“Fish swimming to the left then right”*

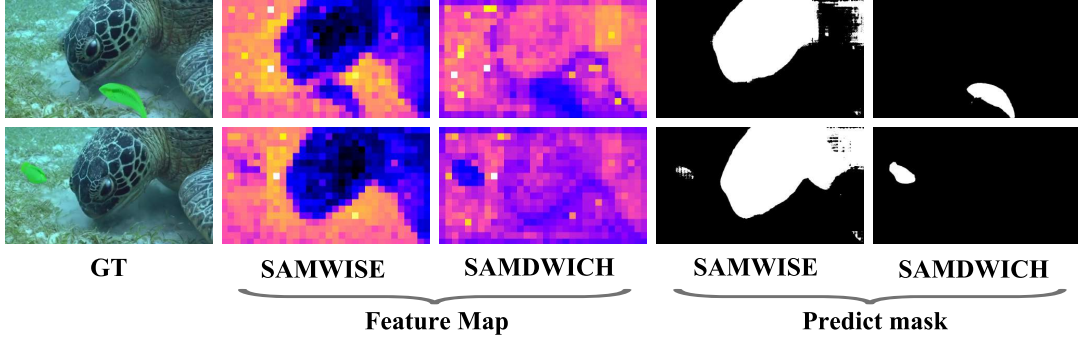


Figure 10: PCA-based **feature maps** and **segmentation results** of SAMWISE & SANDWICH.



Figure 11: An example of a failure case.

criminative, text-aligned representations at the object level. These results clearly show that effective temporal grounding and object-aware training significantly enhance the model’s ability to align visual features with linguistic expressions.

**Qualitative Results** Fig. 12 presents qualitative comparisons between our proposed model, SANDWICH, and existing state-of-the-art RVOS models, SAMWISE and GLUS, on the MeViS dataset. In the first example, SAMWISE incorrectly segments both monkeys in response to the expression “jumping to left,” indicating a lack of moment-aware reasoning. GLUS initially segments the correct object, but fails to maintain consistency, eventually highlighting an unrelated regions. In contrast, SANDWICH accurately segments the referred object throughout the entire sequence by leveraging its moment-aware design and object-level supervision. In the remaining two examples, both SAMWISE and GLUS continue to rely on static appearance cues—such as the presence of a monkey or a rabbit—rather than understanding the motion described in the expression. These results demonstrate that, unlike prior models, SANDWICH effectively grounds language to visual motion by incorporating a moment-aware approach and fine-grained guidance.

## A.5 Limitations

Our SANDWICH framework introduces a moment-aware approach for RVOS, where training is performed using text-relevant frames to achieve precise video-text alignment. This

stands in contrast to prior methods that sample frames randomly, often including ones unrelated to the expression, which can degrade grounding performance. By focusing on temporally aligned frames, our method learns to better associate visual content with language. However, this training strategy introduces a practical limitation: during inference, the model requires knowledge of which temporal segments are relevant to the given expression in order to accurately localize the referred object. Without such information, its grounding capability may decline. As a result, an additional moment retrieval step—using VLMs or a moment retrieval model—is required to identify and select the most relevant segments prior to inference.

A further limitation arises when a single referring expression describes multiple temporally separated actions involving the same object, as shown in Fig. 11. Since SANDWICH uses a single expression-level feature to attend over the entire video, it can struggle to consistently localize the object across distinct action spans, especially when one action visually dominates. This reflects a challenge in handling fine-grained temporal compositionality in multi-action expressions.

While this reliance adds overhead, our method still achieves significantly higher performance than existing approaches when accurate moments are available. This supports our core claim that moment-aware training enables more effective video-language grounding and leads to robust RVOS across diverse scenarios.

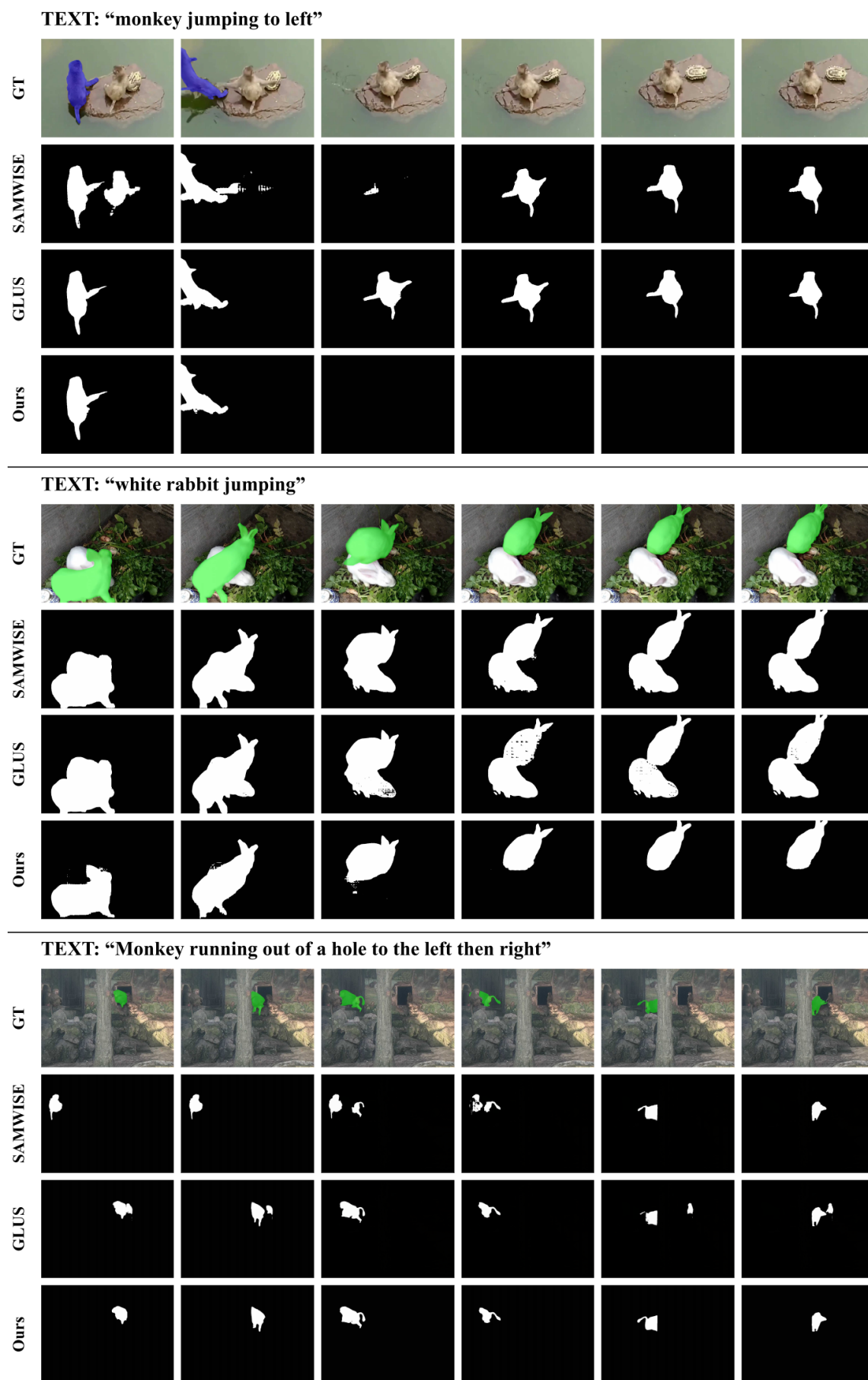


Figure 12: Comparison of qualitative results.